The Effect Of Pitting Corrosion On The Position Of Aircraft Structural Failures

B.R. Crawford, C. Loader and P.K. Sharp
DSTO Air Vehicles Division, PO Box 4331, Melbourne Victoria, Australia, 3207

ABSTRACT: Corrosion has been shown over the last decade to significantly reduce the structural integrity of aircraft as they age. Previous work at DSTO has shown that pitting and exfoliation corrosion are particularly deleterious to aircraft structural integrity. In addition to reducing fatigue endurance, pitting also increases the surface area of the component over which fatigue failures can occur. This paper reports the results of a Monte-Carlo model of this phenomenon, which has been labelled 'corrosion criticality'. This model concentrates on the effect of the pit spatial density and position on the endurance of a fatigue coupon designed to mimic a simple aircraft component. The study's results show that pitting increases the area of the coupon over which failures can occur.

1 INTRODUCTION

The structural integrity of aircraft is based upon design practices in which the fatigue critical sections of components are identified either during design or as part of a teardown after full-scale fatigue testing, with the aim of preventing fatigue failures within the design life of the aircraft type. Pitting corrosion, however, creates damaged regions which are not necessarily located in the nominally fatigue critical regions. In-service experience has shown that fatigue cracks initiated from corroded regions can grow to failure within the aircraft's design life [Cole et al., 1997]. This greatly complicates the inspection of aircraft by enlarging the surface area of the aircraft that must be examined to ensure continued structural integrity.

The practices described above work because it is reasonable to assume that the size of intrinsic defects, such as constituent and second phase particles, is approximately the same throughout the structure of an aircraft. This means, as a consequence of the definition of ΔK and the nature of fatigue crack growth, that only the location of the defect, which controls the stress and, therefore, stress intensity factor, will have an effect. However, the introduction of corrosion into the structure changes this by introducing a set of defects with a completely different and significantly larger size distribution. As a consequence both the defect's size and position become critical. This means that a large defect, such as a corrosion pit, in a low stress region may reduce fatigue life to the same extent as a small defect in a high stress region. This causes the number of critical regions in an aircraft to increase, potentially enlarging the area of an aircraft's structure requiring inspection. This behaviour has been observed in research conducted at DSTO [Mills et al., 2002; Sharp, 2003]

2 THE MONTE CARLO METHOD

As stated above the work reported here is based upon a Monte Carlo simulation. The Monte Carlo method is a means of numerically solving problems, such as integration, that were not amenable to analytical solution [Metropolis and Ulam, 1949]. An outline of the Monte Carlo method may be found in Ayyub et al [Ayyub and McCuen, 1995]. In its simplest form, uniformly distributed random numbers are transformed using some model of the process being studied. The result of this transformation, which in the current case is a fatigue life, is then compared against some 'limit state criteria' to determine if the results fall within the range of interest for the problem being studied. In the current case the limit state criteria was defined as the defect that gave the shortest fatigue life. The principal advantage of the direct Monte Carlo method is that it can be applied to any problem for which a numerical representation can be formulated. However, the variance of its results is proportional to $\sqrt{N}$, where N is the number of repeats. When very low probabilities of the limit state function are being assessed the number of repeats

consequently becomes extremely large. A series of variance reduction techniques have been formulated to overcome this. These include importance sampling, stratified sampling, Latin hypercube, adaptive sampling and the response surface method [Ayyub and McCuen, 1995]. These methods work by simulating the limit state function which allows the Monte Carlo simulation to concentrate on estimates in the vicinity of the correct solution. This greatly reduces the number of repeats required to reach a given level of certainty. However, these methods must be applied carefully to avoid incorrect estimates of the limit state.

3 EXPERIMENTAL DETAILS AND RESULTS

3.1 Development of corrosion protocol

At this stage the experimental work concentrated on the development of a realistic corrosion pitting distribution for input to the criticality model. The underlying corrosion protocol was developed by swabbing four coupons of 60 mm by 10 mm dimensions with a 3.5wt% aqueous solution of NaCl. These coupons were ground to a 1200 grit finish using silicon carbide paper prior to corrosion to activate the material's surface. The coupons were then placed in a high humidity (RH > 80%) environment for periods of 1, 2, 4, 7 and 14 days to allow corrosion pits to develop. At the end of these times the coupons were removed from the high humidity environment and washed with ethanol to remove the corroding solution. The coupons were then mounted in a Reichert Jung Polycut E ultra-miller for serial sectioning. The surface of each coupon was divided into 9 regions of equal area. Serial sectioning was used to identify the largest pit in each of these regions. Successive 10 μm slices of material were removed until all evidence of pitting in a region had disappeared. These depth data were then used to determine an extreme value distribution for largest pit size. Given that this sectioning was conducted on coupons corroded for several different durations this allowed a relationship between deepest pit size and corrosion period to be established. Largest pit size was used in favour of mean pit size as, given an equal stress, the largest defect will typically initiate the fatigue crack that leads to final fracture.

3.2 Maximum pit size distribution

The pit size distributions obtained for seven and fourteen days exposure are shown in Figure 1 as probability and cumulative density functions. These distributions were calculated using an extreme value statistics approach based on the exponential distribution [Castillo, 1988]. Extreme value statistics greatly reduce the number of observations required to obtain a size distribution. Figure 1 shows the predicted largest pit size distribution based on a corrosion strike 2 mm wide and 196 mm long. Examination of parts (a) and (b) of this figure shows that the median pit size increased with increasing exposure time. Note also that the size range of the distribution also increased.

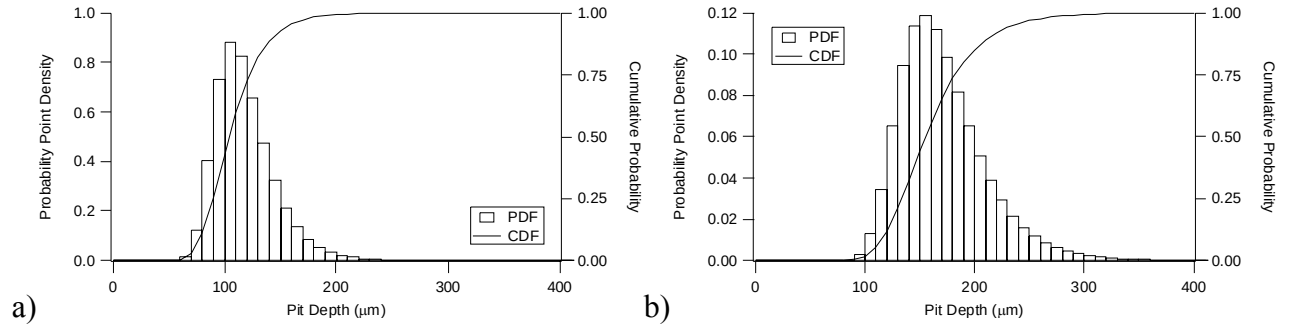

Figure 1: Point (PDF) and Cumulative Density Functions (CDF) of maximum pit depth in 7010-T7651 after (a) 7 days and (b) 14 days exposure in humid air. Distributions were calculated using the exponential distribution function.

4 MODELLING DETAILS AND RESULTS

4.1 Details of criticality model

The structure and algorithm of the criticality model are illustrated in Figure 2. Note that the model is based on the Monte Carlo method which has been implemented without any of the variance reduction techniques described above. The purpose of the model is to simulate the effect of pitting corrosion on the spread of fatigue failures along the surface of a simple fatigue coupon. Corrosion is assumed to occur as "corrosion strikes" which are regions in which pitting corrosion has occurred. In practice such corrosion strikes typically occur due to the failure of the paint system covering the region of a component that has corroded.

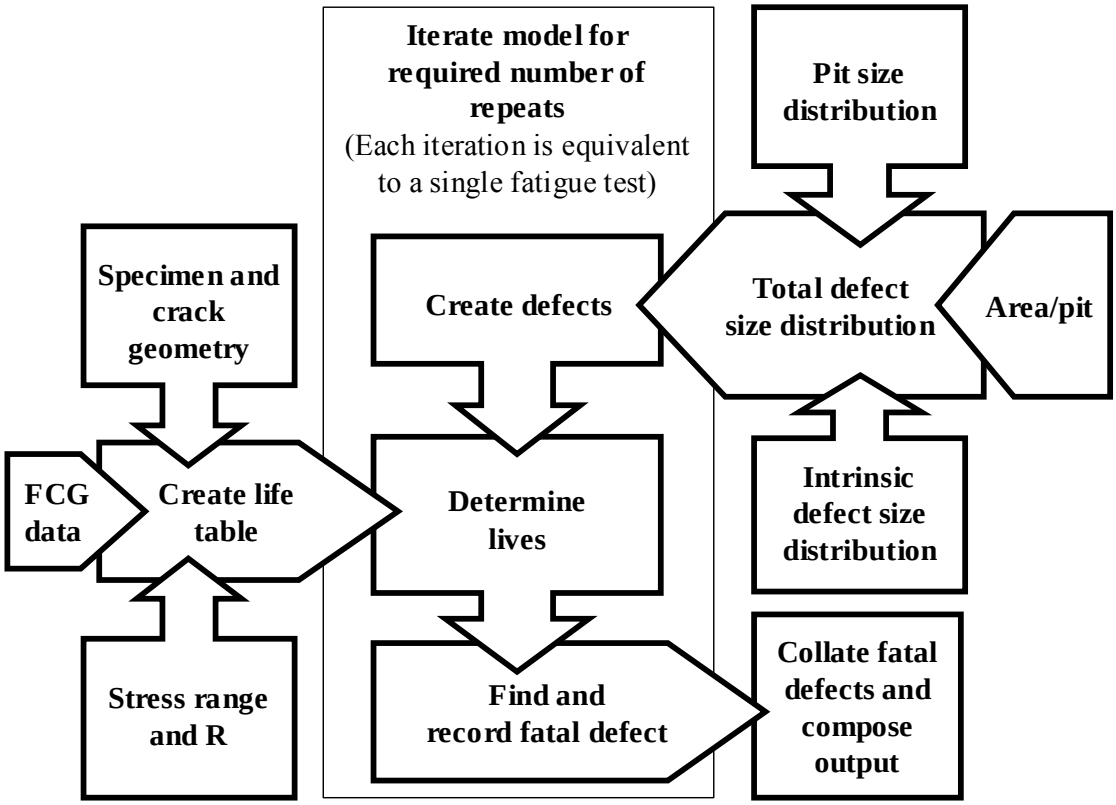

Figure 2: Structure of criticality model showing the model's various inputs and the underlying algorithm.

To simulate pitting corrosion the model requires inputs detailing the material properties of the material, the applied loading and the size of both the intrinsic defects and the pits in the material. These inputs are:

- **Coupon geometry:** This is expressed in terms of a finite element solution of the stress along the longitudinal axis of symmetry of the coupon to which a polynomial equation was fitted. This allowed the stress at any position along the coupon to be estimated as a function of distance from the middle of the gauge-section. The coupon design is shown in Figure 3(a).
- **Fatigue crack growth data:** The fatigue crack growth data to be published in Crawford et al [Crawford et al., 2004] were used to create a lookup table of fatigue lives as a function of defect size (expressed as defect radius in microns) and applied maximum stress (in MPa). Fatigue lives above 3.5×10^6 cycles were considered to be infinite. A load ratio (R) of 0.1 and a semi-circular crack shape was assumed. The AFGROW fatigue life modelling program was used to create this table [Harter, 2003b; c] using the program's COM interface [Harter, 2003a].

- **Maximum Stress range:** This fell within the range of stresses allowed by the underlying fatigue crack growth data. The upper value of maximum stress used was always less than the material's yield stress.
- **Pit size distribution:** This was obtained experimentally by serial sectioning of corroded surfaces of as-machined 7010-T7651. The pit size distribution is illustrated in Figure 1. The 7-day pit size distribution was used in this paper. It was assumed that there was no size difference between a corrosion pit and the fatigue crack producing an equivalent life.
- **Corrosion strike length:** This is the length of the corroded region on each coupon. This increases the number of pits on the coupon but does not change the linear density of pits. Note that there is a stress gradient along the corrosion strike.
- **Corrosion strike width:** This is the width of the corroded region on each coupon. Increasing the width of the corrosion strike increases the linear density of pits and the total number of pits. Given that the stress is effectively constant across a corrosion strike this should only affect the spread of fatigue failures.
- **Corrosion strike centre:** This is the centre of the corroded region, which represents the position of the corrosion strike on the coupon's surface. This position can either be allowed to vary randomly along the coupon's gauge length (within a selected range) or can be set to a specific value (such as in the centre of the coupon's gauge section).
- **Area per pit:** defines the area in which the largest pit is being estimated. That is, if the area per pit is 20 mm^2 then the pit size distribution (which is defined by a exponential distribution function) will return the distribution of largest pits in this area. It also determines the number of pits on a coupon as a percentage of the total defects within the corrosion area.
- **Intrinsic defect size distribution:** This is the size distribution of the intrinsic defects, which was determined by microscopic examination of polished sections of the material. It was assumed that the intrinsic defect size and equivalent fatigue crack size were identical.

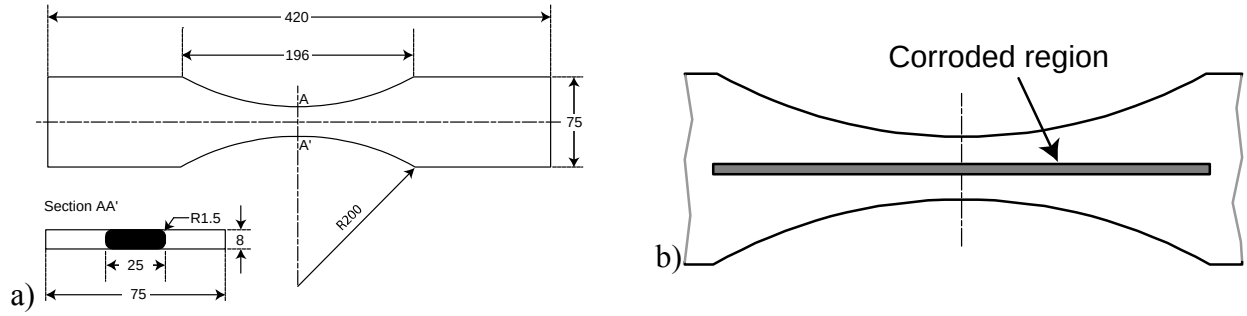

Figure 3: (a) Coupon geometry (b) position of corrosion region

These inputs are used to simulate a corroded fatigue coupon (Figure 3(a)) using the following algorithm. Defects on the coupon's surface are generated using cumulative particle size histograms (e.g. Figure 1) using the inverse transformation method [Ayyub and McCuen, 1995] while defect position is randomised uniformly along the coupon's gauge. Defect sizes within the corrosion strike are simulated using a combined (pit and intrinsic defects) size histogram. Those outside the corrosion strike use only the intrinsic defects size distribution. The size and position of the resultant defects and pits are then compared with a lookup table of fatigue life as a function of these inputs. The defect with the shortest life is selected as being the "fatal" defect and its size and position recorded. The model then repeats this process for the required number of iterations. The model's output is a scatter graph showing the relation between pit size and failure location.

4.2 Model results

4.2.1 Effect of corrosion strike length

The model was run using the parameters listed in Table 1. The fatigue limit was selected to eliminate spurious runouts due to the lack of data in the lower end of the fatigue crack growth curve collected for the material.

Table 1: Model parameters used to evaluate the effect of corrosion strike size.

σ_{max} (MPa)	R	Area per pit (mm^2)	Strike width (mm)	Strike length (mm)	Defect density (mm^{-2})	Fatigue limit (cycles)	Repeats
380	0.1	20	5	0, 10, 50, 100	30	290,000	5000

Figure 4 shows the results for corrosion strike lengths of 0 (no-corrosion), 10 mm, 50 mm and 100 mm. It also shows the domain in which a fatigue failure is possible at the loading and runout conditions listed in Table 1. Part (a) of this figure shows the case where there is no corrosion. Therefore, fatigue failures will be due to intrinsic particles, which due to their small size can only fail within the central high stress region (see the normalised stress profile in Figure 4(a)). This produces the observed narrow distribution of failures. Note also that this distribution of failures is far narrower than those that are theoretically possible.

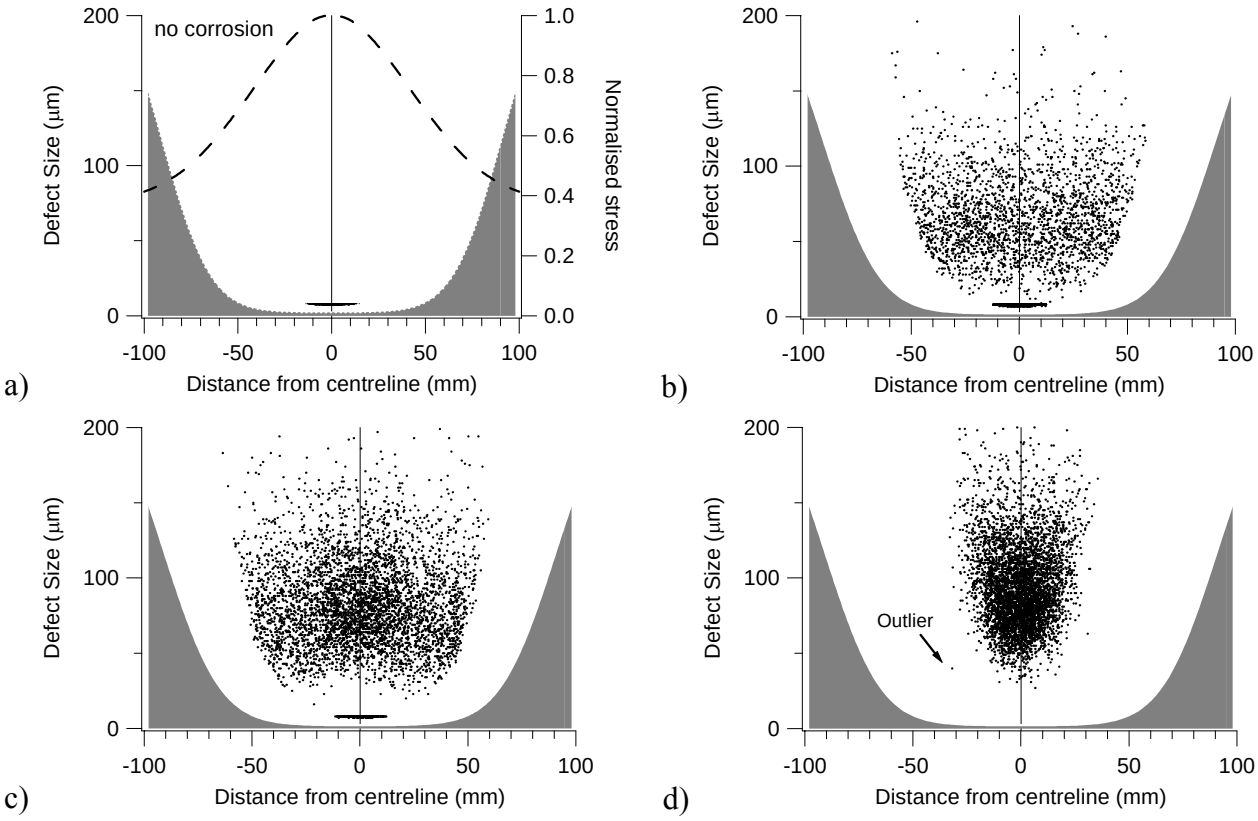

Figure 4: Scatter graphs showing distribution of failures due to fatigue cracks initiated from intrinsic particles and pits with pit strike lengths of (a) 0 mm (no corrosion), (b) 10 mm, (c) 50 mm and (d) 100 mm. The pit strikes were all 5 mm wide and the area per pit was 20 mm^2. The shaded region in each graph is the domain in which a fatigue failure is not possible at the applied maximum stress (380 MPa) and fatigue limit (290,000 cycles). Note that this domain is the same for all cases shown in this figure. The dashed line in part (a) is the longitudinal stress in the coupon normalised by its maximum value at the coupon's centre.

The introduction of relatively short corrosion strikes (10 mm long) positioned randomly along the gauge length (see Figure 4(b)) increases the spread of fatigue failures to ±60 mm. Once a small corrosion strike is introduced to the coupon there is a good chance that this strike will (a) contain a large corrosion pit and (b) that this pit will be located outside the region of the coupon where intrinsic failures occur. Further increases in the corrosion strike length (see Figure 4(c) and (d)), however, cause the fatigue critical region to contract again. This occurs because of the increased probability of a large defect occurring in the coupon's central, high stress region. This is particularly apparent in the case of a 100 mm long corrosion strike (Figure 4(d)). Despite this, failures can still occur at large distances from the high stress region, as shown by the outlier in Figure 4(d). The probability of these, however, is extremely low due to the typically high density of pits in the high stress region.

4.2.2 Effect of corrosion strike width

Having investigated the effects of corrosion length, we now studied the effect of corrosion area width which controls the lineal density of pits on the coupon. Pit lineal density was defined as the number of pits per unit length along the coupon's gauge length. It is controlled by the exponential pit size distribution described above and the width of the corrosion region. At a corrosion region length of 196 mm and given the pit size distribution in Figure 1, a 0.1 mm wide corrosion region will produce one pit of fatigue critical size per coupon (i.e. iteration of the Monte Carlo model).

Figure 5(a) shows the effect of a single corrosion pit on the spread of fatigue failures. The spread of failures is far wider than for an uncorroded sample (cf. Figure 4(a)) in which only intrinsic defects are present. Increasing the width of the corrosion area to 1 mm, which gives an average of 10 corrosion pits per coupon, however, decreases the spread of fatigue failures. For example, a corrosion pit of 100 μm size located ±50 mm from the coupon's middle can cause failure at a corrosion area width of 0.1 mm but is very unlikely to cause failure at a corrosion area width of 1 mm. This is because the increased number of pits per coupon means that there is likely to be a pit of shorter life towards the middle of the coupon.

This narrowing of the spread of fatigue failures is caused by interaction of the increased number of pits per coupon due to an increase in corrosion area width with the change in stress with distance from the coupon's middle (see Figure 4(a)). Removal of the stress gradient would eliminate this effect but only because the position of fatigue failures would become completely independent of corrosion. That is, the introduction of corrosion into a constant stress structure would only decrease its life and would not affect the position of failures. Further increases in corrosion area width as shown in Figure 5(c) and (d) further concentrates failures in the coupon's high stress region.

Note that an increased corrosion area width also eliminates failures due to intrinsic defects and increases the minimum size of a critical defect. This is due to the increased number of pits on the coupon increasing the likelihood of a pit with a shorter life being at a similar distance from the coupon's centre. This is the same mechanism that narrows the spread of failures with increased corrosion area width. Failures from intrinsic defects are eliminated simply because the intrinsic defects in this simulation are smaller than the pits.

4.2.3 Frequency of pitting failures as a function of fixed corrosion strike position

In the previous two sections the position of the corrosion strike was allowed to vary randomly. While this allows the effect of corrosion strike size to be modelled a comparison with experimental results is impractical because of the large number of iterations in the model (5000) and the difficulty of creating "random" corrosion strikes. For these reasons the model's prediction of the proportion of failures due to pitting and intrinsic defects was studied as a function of the position of a deliberately placed corrosion strike. The corrosion strike was set to a length of 10 mm a width of 5 mm and the position was varied along the coupon's gauge length. Figure 6 shows the output of the model under these conditions. The

number of failures due to pitting increases as the corrosion strike placement approaches the centre of the coupon, but intrinsic defect failures always occur, as there exists a small chance that no corrosion pits will occur on any given coupon. The model determines the combined distribution of defects within a corrosion strike, which takes into account the probability of occurrence. A defect is assigned a position and if this falls into the corrosion strike, it is assigned a defect size based on the combined distribution. There are a large number of defects with each having only a small probability of its defect size coming from the pitted distribution. With a large number of runs, occasionally none of the defects will result in pitting. As the corrosion strike moves away from the centre, the chance of having no defects large enough to cause failure occurring within the corrosion strike increases. Intrinsic failures however, continue to occur. Such a prediction can be tested experimentally though the number of repeat coupons will clearly be several orders of magnitude less. Coupons are currently being prepared to perform such an experimental comparison.

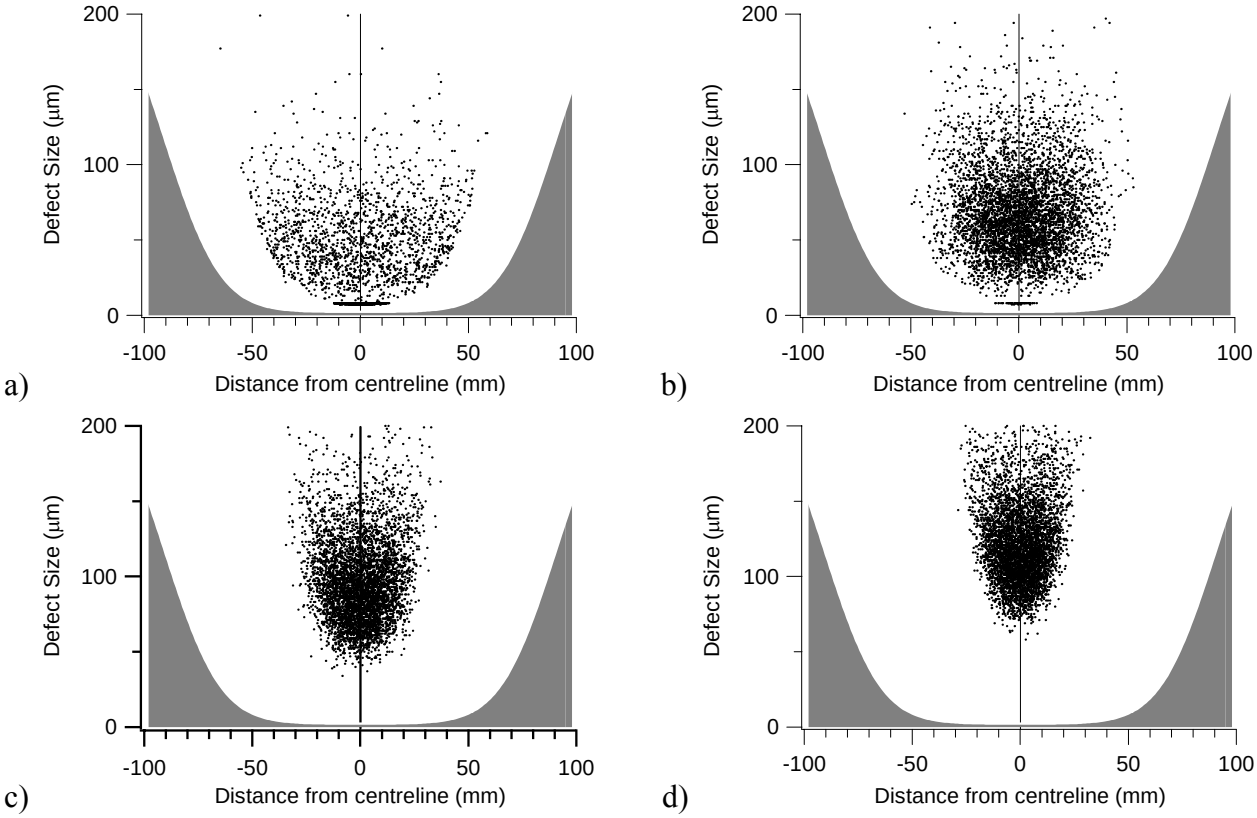

Figure 5: Scatter graphs showing distribution of failures due to fatigue cracks initiated from intrinsic particles and pits with corrosion strike widths of (a) 0.1 mm, (b) 1 mm, (c) 5 mm and (d) 20 mm. Corrosion strike length is 196 mm in all cases. The shaded region in each graph is the domain in which a fatigue failure is not possible at the applied maximum stress (380 MPa) and fatigue limit (290,000 cycles). Note that this domain is the same for all cases shown in this figure.

5 CONCLUSIONS AND FURTHER WORK

This paper represents the second report of research being conducted at DSTO into modelling the effect of pitting corrosion on the spread of fatigue critical regions in aircraft structural components. In the process of doing this several simplifying assumptions have been made. One of these was to assume that a surface defect acts as a crack of the same size. Despite these assumptions, a range of useful observations has been made.

As shown by this model, corrosion criticality has implications for the management of the structural integrity of aircraft. The spread of fatigue critical regions due to pitting corrosion means that those regions of aircraft, which were considered to be safe by design, may not actually be safe once corroded. There are at least two scenarios to be considered. In the first, the corrosion of low stress regions of a

fatigue critical component means that the area of that component requiring inspection will need to be increased if safe operation is to be ensured. This increases the cost of maintenance and, consequently, the cost of fleet operations. The second scenario is where the corrosion of a durability component (i.e. a component that is designed with a fatigue life far in excess of the aircraft) may cause it to fail during the life of the aircraft. Such a failure could prevent the safe operation of the aircraft and may lead to expensive repairs.

The model is yet to be experimentally validated. It is planned to conduct a series of fatigue tests on coupons that have been selectively corroded to determine if the effects observed in the results of this model are observed under experimental conditions. A direct test of the spread of failures shown in this paper (see Figure 4 and Figure 5) is not possible due to the large number of repeats that would be required.

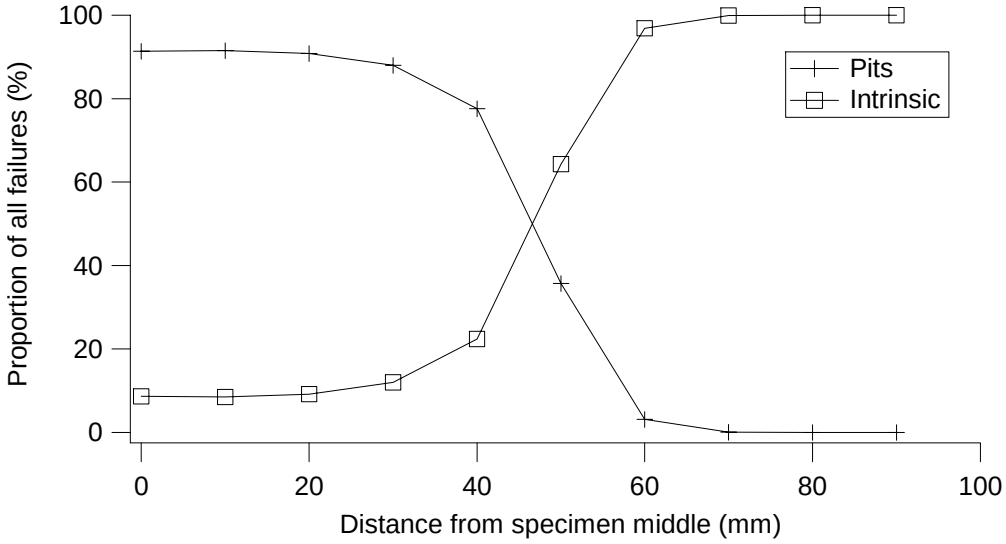

Figure 6: Proportion of failures due to intrinsic defects and pits.

ACKNOWLEDGEMENTS

The authors would like to thanks Claude Urbani of CSIRO for the FEA model used in this work.

REFERENCES

Ayyub, B. M. and McCuen, R. H., Simulation-Based Reliability Methods. *Probabilistic Structural Mechanics Handbook*. C. Sundararajan. New York, Chapman and Hall**:** 745 (1995).

Castillo, E., *Extreme Value Theory in Engineering*. San Diego, Academic Press (1988).

Cole, G. K., Clark, G. and Sharp, P. K., The implications of corrosion with respect to aircraft structural integrity. Melbourne, DSTO**:** 120 (1997).

Crawford, B. R., Loader, C., Ward, A. R., Urbani, C., Bache, M. R., Spence, S. H., Hay, D. G., Evans, W. J., Clark, G. and Stonham, A. J., "The EIFS distribution for anodised and corroded 7010-T7651 under constant amplitude loading." *Fat. Fract. of Engineering Mats. Struct* Submitted for publication (2004).

Harter, J., AFGROW COM Server Manual, USAF WPAFB. **2003** (2003a).

Harter, J., AFGROW Program, USAF WPAFB. **2003** (2003b).

Harter, J., AFGROW User's Guide, USAF WPAFB. **2003** (2003c).

Metropolis, N. and Ulam, S., "The Monte Carlo Method." *Journal of the American Statistical Association* **44**: 335-341 (1949).

Mills, T., Sharp, P. K. and Loader, C., The Incorporation of Pitting Corrosion Damage into F-111 Fatigue Life Modelling. Melbourne, DSTO**:** 178 (2002).

Sharp, P. K., ECS Modelling of 7050 Aluminium Alloy Corrosion Pitting and its Implications for Aircraft Structural Integrity. Melbourne, DSTO (2003).